Original Article
Histological validation of frequency domain optical coherence tomography for the evaluation of neointimal formation after a novel polymer-free sirolimus-eluting stent implantation

Qiang Fu[1], Hongyu Hu[1], Wei Chen[1], Zhixu Tan[1], Li Li[2], Dezhao Wang[1], Buxing Chen[1]

[1]Department of Cardiology, Beijing Tiantan Hospital, Capital Medical University, Beijing, China; [2]Department of Pathology, National Center for Cardiovascular Disease, China and Fuwai Hospital, Chinese Academy of Medical Sciences and Peking Union Medical College, Beijing, China

Abstract: Novel polymer-free drug-eluting stents have been developed to reduce polymer-related adverse events. However, neointimal coverage after polymer-free DES implantation is unclear and validation between optical coherence tomography (OCT) and histology is required. Sixteen polymer-free sirolimus-eluting stents were randomly implanted into coronary arteries of 8 normal swine. OCT and histological measurement were conducted at 3 or 6 months after stent placement. For quantitative measures, lumen area, stent area, neointimal area and neointimal thickness were validated in every single OCT and histology matched cross-section. Moreover, for qualitative analysis, OCT signal patterns of neointimal tissue were classified as homogeneous, layered and heterogeneous patterns based on optical intensity and backscatter pattern and peri-strut inflammation was also determined by histology. In total, 70 OCT and histology matched cross-sections were analyzed. At quantitative analysis, good correlations and agreements were found in the measurement of lumen area (ICC = 0.67, P<0.001), neointimal area (ICC = 0.89, P<0.001) and neointimal thickness (ICC = 0.94, P<0.001) except for stent area (ICC 0.19, P = 0.13) between OCT and histology. At qualitative analysis, lymphocyte infiltrations of peri-strut were more frequently seen in heterogeneous sections than in homogeneous sections (10/14 sections, 71.4% vs. 12/50 sections, 24%; P = 0.003). In conclusion, OCT has proper correlation and agreement with histology in assessment of neointimal formation and heterogeneous neointima assessed by OCT may also be associated with peri-strut inflammation detected in histology after polymer-free sirolimus-eluting stents implantation, supporting the use of OCT to evaluate neointimal coverage after polymer-free stent implantation in clinical practice.

Keywords: Polymer-free, optical coherence tomography, histology, neointima

Introduction

Although drug-eluting stent (DES) is deemed to be the effective interventional strategy for coronary artery disease, in-stent thrombotic event has become a critical concern with the increasing clinical use of DES [1-3]. In order to solve the issue, several polymer-free DESs have been developed and also proved to be a feasible method to decrease polymer-related adverse events [4-6]. Optical coherence tomography (OCT) is an ideal intravascular imaging tool to quantitatively evaluate neointimal coverage and stent healing after stent implantation owing to its high resolution, which is 10 times higher than intravascular ultrasound [7-10]. Re-cently, second-generation frequency domain OCT (FD-OCT) is widely used with a substantially increased speed of image acquisition compared with first-generation time-domain OCT [11]. Although previous studies showed that OCT imaging had high correlation with histology for assessment of in-stent restenosis and neointimal formation [7, 12, 13], a histological validation of FD-OCT for the evaluation of in-stent neointimal coverage after polymer-free DES implantation has not been fully investigated. Hence, we carried out an animal study to investigate the validation between FD-OCT and histology measurements in quantification of neointima formation of polymer-free DES.

Table 1. Comparison of the quantitative parameters between FD-OCT and histological measurements

	FD-OCT	Histology
Lumen area mm^2	2.4±0.7	2.0±0.5
Stent area mm^2	3.9±0.5	3.6±0.5
Neointimal area mm^2	1.5±0.5	1.7±0.6
Neointimal burden %	37.8±13.1	44.8±14.6
Neointimal thickness μm	261.2±109.5	269.8±107.2

Data are reported as mean ± SD. FD-OCT frequency domain optical coherence tomography.

Materials and methods

Nano polymer-free sirolimus-eluting stent

Nano (Lepu Medical Technology, Beijing, China) polymer-free sirolimus-eluting stents (SES) are made of stainless steel and the sirolimus concentration is 1.2 μg/mm^2. There are a large number of pores with a diameter of 100 nm×1 μm on the stent struts and sirolimus is released slowly via the nano-porous surface of the stent platform.

Animal study design

A total of 8 juvenile Chinese swine with a body weight of 20 to 30 kg were used in this study. Sixteen nano polymer-free SES were randomized to implantation into the right coronary artery (RCA), left anterior descending (LAD) or left circumflex (LCX) coronary artery with two stents in each swine model (one stent per vessel). Three days before coronary procedure, animals were given 300 mg of aspirin and 75 mg of clopidogrel. Thereafter, antiplatelet therapy of 75 mg clopidogrel and 100 mg of aspirin was administered daily throughout the study in all animals. Coronary catheterization was performed after the administration of intravenous heparin (5000 u). Baseline angiography was acquired and all stents were implanted with a vessel overstretch of 10-20% compared with the reference vessel diameter to induce a moderate vessel injury and promote neointimal formation. Stents of 14, 15 or 18 mm length and diameters of 2.5, 2.75 or 3.0 mm were implanted according to the coronary artery size. FD-OCT follow-up study was performed at 3 and 6 months after stent implantation (eight stents/four pigs each time point). The study protocol was approved by the institutional animal care and use committee at Beijing Tiantan Hospital.

FD-OCT acquisition and analysis

FD-OCT imaging was performed using the C7-XR OCT intravascular imaging system (Lightlab Imaging, Inc., St Jude Medical, USA). During FD-OCT image acquisition, a continuous non-occlusive contrast-saline mixture as a flush was administrated to replace coronary blood flow and automatic pullbacks were performed at a rate of 20 mm/s and 100 frames/s. Offline OCT analysis was performed with Light Lab Imaging software.

For quantitative analysis, cross-sectional OCT images were analyzed at 1-mm longitudinal steps throughout the pullback from distal stent edge to proximal stent edge. OCT images were excluded from the analysis if stent struts were not visible on the screen, bifurcation cross-sections with side branches, or residual blood was mistaken for neointimal tissue. The lumen and stent were manually traced and stent struts were positioned manually in the center of the stent strut which showed a bright "blooming" appearance [14]. The following parameters were measured: lumen area (defined as the delimiting contours of the lumen), stent area (identified by circumferential area limited by the contours of the struts), neointimal area (stent area-lumen area), neointimal burden (mean neointimal area/mean stent area ×100%). To analyze a neointimal thickness, the distance from the center of each stent strut to the luminal border was measured in the direction of the center of gravity. Quantitative analyses of all OCT images were performed by two independent investigators (F.Q. and T.Z.) who were masked to the angiographic data and clinical presentations. Inter-observer agreement was determined by calculating values for differences in measurements of neoinitimal area and neoinitimal thickness analyzed by 50 cross-sectional images without artifacts.

For qualitative analysis, the OCT signal patterns of neointimal tissue were categorized into three patterns based on Gonzalo's classification: homogeneous, layered and heterogeneous patterns [15]. The homogeneous pattern is defined as neointimal tissue with uniform optical properties without focal variation in the backscattering pattern. The heterogeneous pattern is defined as neointimal tissue with focally changing optical properties and various backscattering patterns, and the layered pattern has concentric layers with different optical properties.
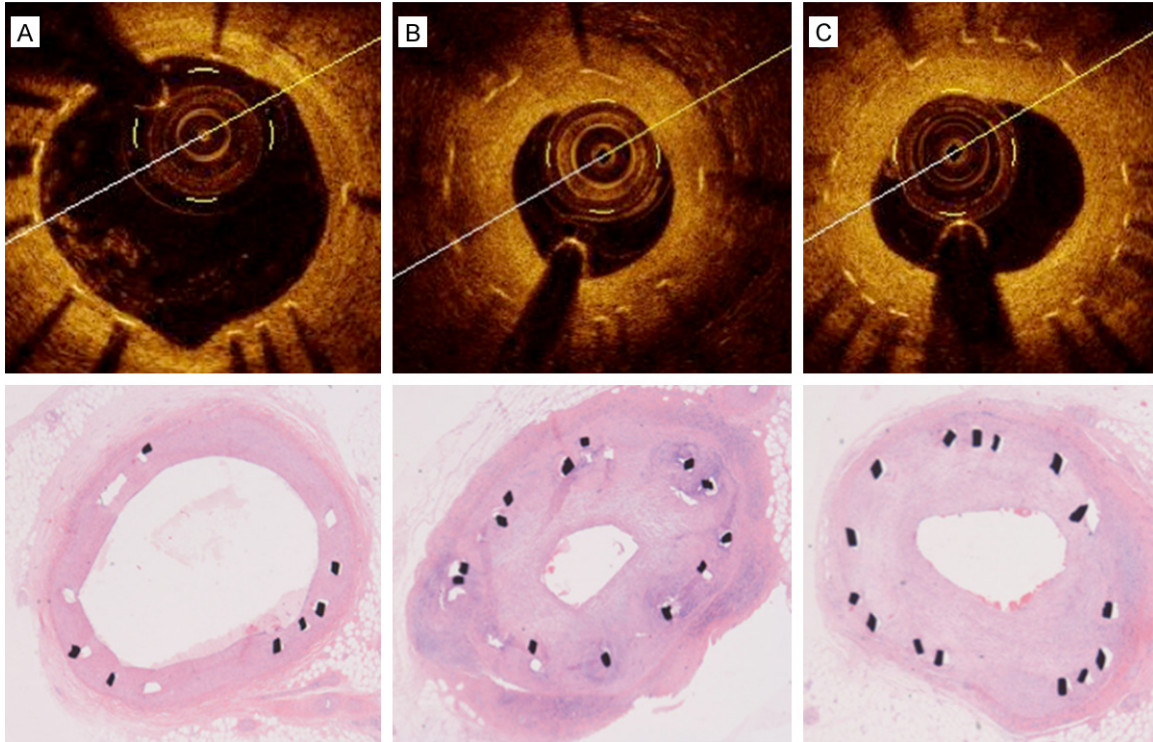
Figure 1. Representative images of FD-OCT and histomorphologic sections (HE stain ×4) at 3 and 6 months after nano polymer-free sirolimus-eluting stent implantation. A. Slight neointimal formation at 3 months; B. Neointimal proliferation (heterogeneous) and strut-associated inflammatory cell infiltration detected by histology at 3 months; C. Significant neointimal proliferation (homogeneous) at 6 months. FD-OCT, frequency domain optical coherence tomography; HE, hematoxylin and eosin.

Histological analysis

All animals were euthanized after follow-up coronary angiography and OCT imaging. Immediately after euthanasia, the hearts were excised and the stented coronary artery segments were then harvested from the heart by careful dissection and fixed by immersion in 10% formalin, dehydrated in a graded series of ethanol, and embedded in methyl methacrylateresin. After polymerization, sections measuring approximately 1.3 mm were sawed from each stent, beginning at the distal stent edge. The artery-stent specimens were cut on a rotary microtome at 100 μm from the proximal through the distal margin of the stent and stained with hematoxylin and eosin as well as elastic Van Gieson stains. There were no histological sections lost due to processing, and all sections were of excellent quality.

The cross-sectional areas including external elastic lamina representing stent area, internal elastic lamina and lumen area of each section were measured. Neoinitimal thickness was determined as the distance between the inner surface of each stent strut and the luminal border in the direction of the center of gravity. Morphometric analysis was performed by ImagePro Plus 6.0 software (Media Cybernetics, Inc. USA).

For qualitative assessment, all sections were analyzed by light microscopy. Stent-associated inflammation and neovascularization identified by microvessels in the neointima were investigated. All histomorphologic analysis was completed by a single independent investigator (L.L.) blinded to the present study.

Statistical analysis

Data are reported as means and standard deviations for normally distributed continuous data or medians with interquartile ranges for nonnormally distributed data. Student's t-test (two-sided) was used for comparison of normally distributed continuous data, and Mann-Whitney U-test (two-sided) was used for the statistical comparison of non-normally distributed continuous data. The association between FD-OCT and histological analysis was calculated using
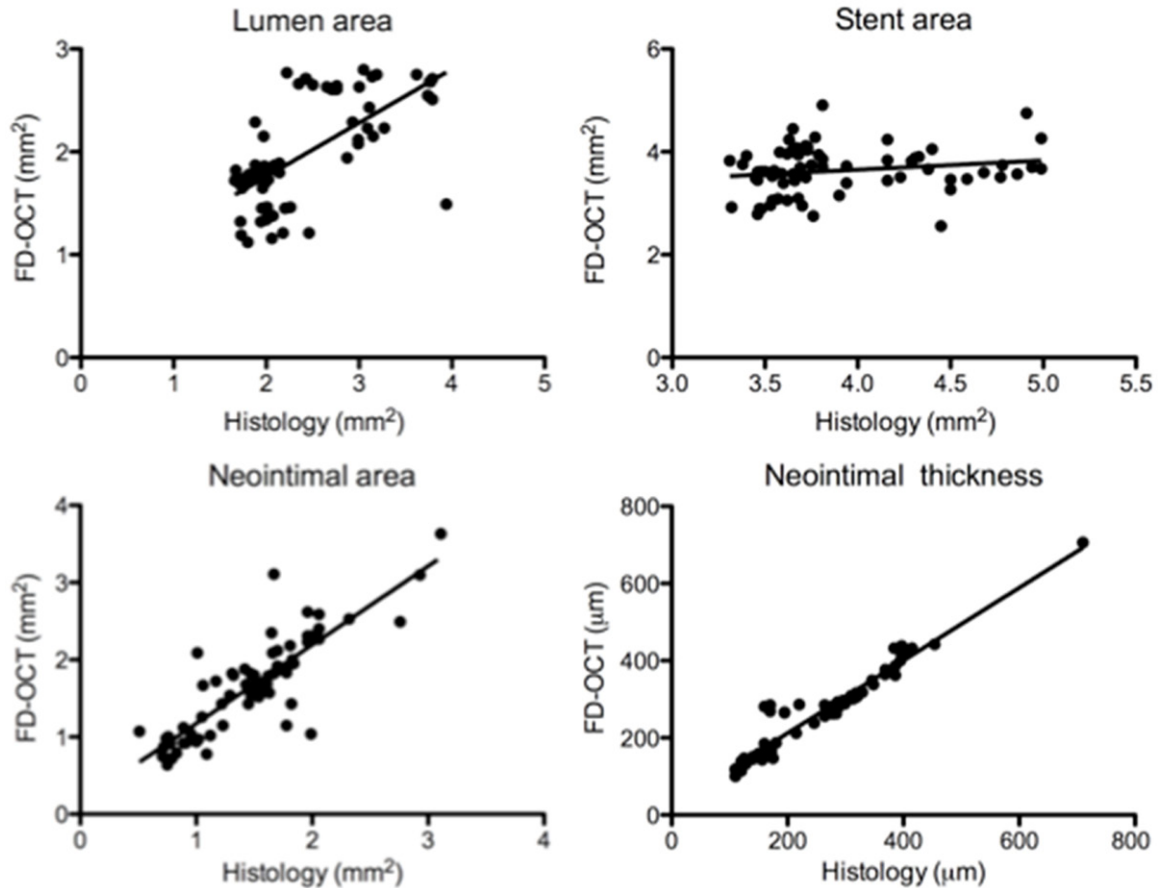
Figure 2. Relation of measurements of lumen area, stent area, neointimal area and neointimal thickness between FD-OCT and histomorphology. FD-OCT, frequency domain optical coherence tomography.

intra-class correlation coefficient (ICC). The agreement between FD-OCT and histological analysis was determined by Bland-Altman plots [16]. Additionally, inter-observer variability for the quantitative OCT assessment was investigated using a kappa analysis. Differences were considered statistically significant at $P<0.05$. Statistical analyses were performed using SPSS 20.0 software (IBM Corporation, Armonk, NY, USA).

Results

A total of 70 OCT and histology matched cross-sections were analyzed in the present study. The quantitative parameters between FD-OCT and histological measurements are shown in **Table 1**. The lumen and stent areas measured by FD-OCT were slightly larger, on average, than those measured by histology. Conversely, FD-OCT measurements have smaller neointimal area, neointimal burden and neointimal thickness compared with histological measure-

ments. Representative images of FD-OCT and histomorphologic sections after Nano polymer-free SES implantation are shown in **Figure 1**.

Inter-observer variability for the quantitative FD-OCT assessment showed good concordance: k = 0.91 for neointimal area, k = 0.81 for neointimal thickness.

Figure 2 showed correlations of quantitative parameters between FD-OCT and histological measurement. Adequate correlations were found in the measurement of lumen area (ICC 0.67, $P<0.001$), neointimal area (ICC 0.89, $P<0.001$) and neointimal thickness (ICC 0.94, $P<0.001$) except for stent area (ICC 0.19, $P = 0.13$). Similarly, the Bland-Altman analysis is shown in **Figure 3**, suggesting that there are good agreements between FD-OCT and histological measurements in terms of lumen area, neointimal area and neointimal thickness except for stent area.
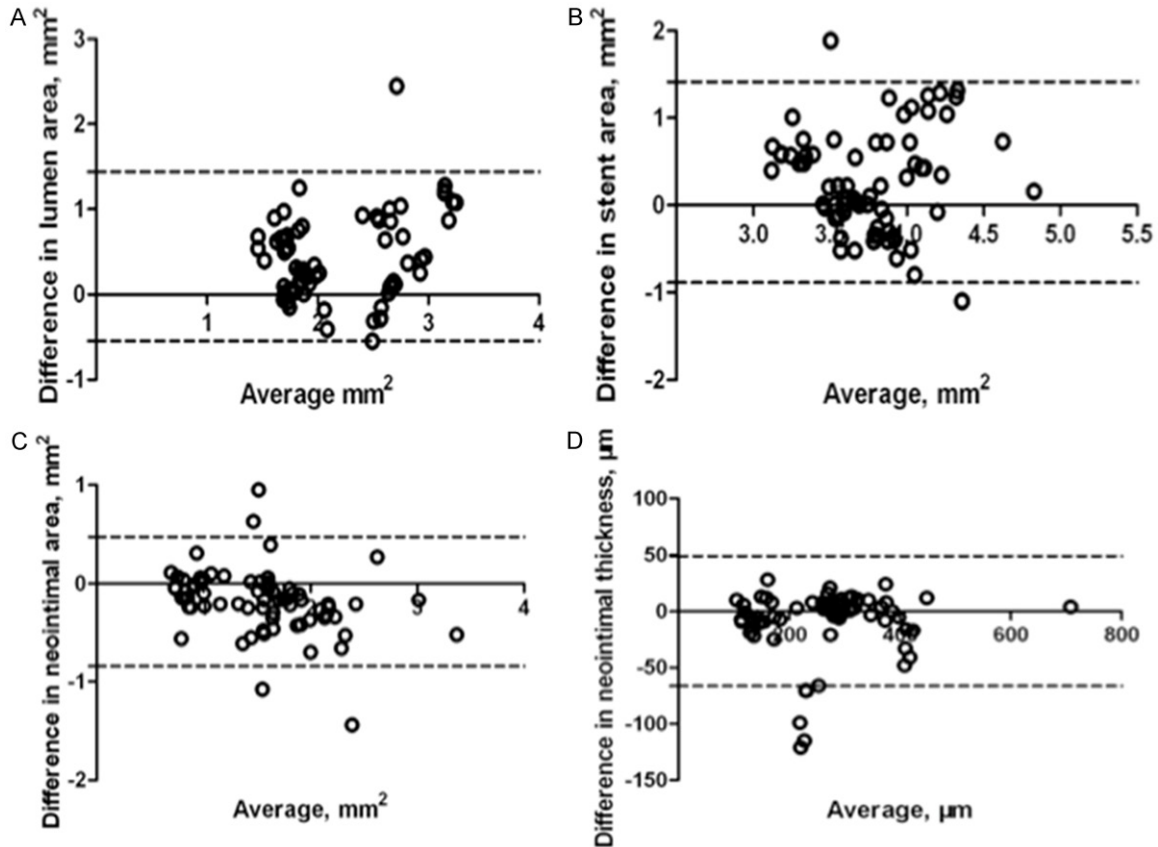
Figure 3. Bland-Altman plot (Dash lines = limit of agreements) are shown demonstrating the agreement between lumen area (A), stent area (B), neointimal area (C) and neointimal thickness (D) measurements obtained by FD-OCT and histomorphology analysis. FD-OCT, frequency domain optical coherence tomography.

As for tissue characteristics of neointima assessed by FD-OCT, 70 OCT and histology matched cross-sections were classified to 50 homogeneous sections (71.4%), 14 heterogeneous sections (20%) and 6 layered sections (8.6%).

Additionally, in histological analysis, lymphocyte infiltrations of peri-strut were observed in 22 OCT and histology matched sections and more frequently seen in heterogeneous sections than in homogeneous sections (10/14 sections, 71.4% vs. 12/50 sections, 24%; $P = 0.003$).

Discussion

The present study demonstrates good agreements between FD-OCT and histological quantitative analysis for the evaluation of neointimal formation after novel nano polymer-free drug-eluting stent in a pig model. Moreover, at qualitative analysis, heterogeneous neointima assessed by FD-OCT may also be associated

with peri-strut inflammation detected in histology.

Recently, FD-OCT has emerged as a novel, highly rapid coronary imaging method for assessing neointimal coverage after coronary stent implantation [17]. Furthermore, according to our previous investigation, OCT can detect different signal intensity and attenuation in different period of in-stent restenosis [18]. However, the accuracy of this imaging method needs to be further evaluated, especially validate with histology. In addition, polymer-free stent has begun to apply increasingly in clinical practice but morphological characteristics of in-stent neointimal tissue assessed by OCT are not still fully investigated.

With respect to quantitative measures, lumen area, neointimal area and neointimal thickness as detected by FD-OCT correlated closely with these parameters as measured by histology, demonstrating an excellent agreement in the present study. However, no significant relation

of measurement of stent area between FD-OCT and histology was found. Moreover, the OCT measurements of lumen and stent area were greater than the same histological measurements in the study, and similar result was also reported by Murata A et al [7]. The differences may be mainly attributed to different method of measurement. In general, histomorphological analysis used as the gold standard defines in-stent neointima as the interval encompassed by the internal elastic lamina and the lumen boundaries in vessel cross-sections, whereas in OCT imaging, the internal elastic lamina cannot be identified and the stent outline is used as a substitute for the calculation of neointimal parameters [19]. Thus, the technical issue may result in differences of some of the measurements between OCT and histomorphology. In addition, vascular tissue shrinkage during histological procedure could be involved [20]. Nevertheless, in the present study, we showed that the quantitative assessment of in-stent neointimal proliferation using OCT is correlated with the measurements from histomorphological analysis, suggesting that OCT can provide precise measurement like histomorphology for in-stent neointimal proliferation due to its high resolution.

On the other hand, FD-OCT measurements seem to be related to histomorphological results in the qualitative analysis. In histomorphological analysis, obvious lymphocyte infiltration of peri-strut was found and more prevalent in heterogeneous structure assessed by OCT, suggesting that heterogeneous neointima may be associated with peri-strut inflammation. Likewise, Tearney GJ et al [21] also investigated the use of OCT for assessing macrophages degradation, demonstrating that the high resolution of OCT may be well suited for identifying macrophages within fibrous caps. However, FD-OCT was still difficult to identified lymphocyte infiltration around stent strut. A possible explanation for the finding is that light attenuation within arterial tissue and strut blooming resulted in a lack of peri-strut tissue detection [7].

Overall, our findings demonstrate that neointimal parameters including neointimal area and neointimal thickness measured by FD-OCT may be substituted for the measurements of histopathology. Moreover, OCT heterogeneous neo-

intima may be associated with peri-strut inflammation detected in histology.

Study limitation

The main limitation of this study was that stents were placed in health pigs without atherosclerotic disease and thus several complex profiles of arterial healing and neointimal formation in human could not be detected. Furthermore, the sample size of animals is small.

Conclusion

Proper correlation and agreement were found in assessment of neointimal formation between FD-OCT and histology as well as OCT heterogeneous neointima might be associated with peri-strut inflammation detected in histology, supporting the use of FD-OCT to evaluate neointimal coverage after polymer-free stent implantation in clinical practice.

Acknowledgements

Disclosure of conflict of interest

None.

Address correspondence to: Dr. Buxing Chen, Department of Cardiology, Beijing Tiantan Hospital, Capital Medical University, 6 Tiantanxili, Dongcheng District, Beijing, China. Tel: 86-10-6709-6572; Fax: 86-10-6709-6572; E-mail: chbux@126.com

References

[1] Stone GW, Ellis SG, Cox DA, Hermiller J, O'Shaughnessy C, Mann JT, Turco M, Caputo R, Bergin P, Greenberg J, Popma JJ, Russell ME; TAXUS-IV Investigators. A polymer-based, paclitaxel-eluting stent in patients with coronary artery disease. N Engl J Med 2004; 350: 221-231.

[2] Finn AV, Joner M, Nakazawa G, Kolodgie F, Newell J, John MC, Gold HK, Virmani R. Pathological correlates of late drug-eluting stent thrombosis: strut coverage as a marker of endothelialization. Circulation 2007; 115: 2435-2441.

[3] Nakazawa G, Finn AV, Vorpahl M, Ladich ER, Kolodgie FD, Virmani R. Coronary responses and differential mechanisms of late stent thrombosis attributed to first-generation sirolimus- and paclitaxel-eluting stents. J Am Coll Cardiol 2011; 57: 390-398.

[4] Hausleiter J, Kastrati A, Wessely R, Dibra A, Mehilli J, Schratzenstaller T, Graf I, Renke-Gluszko M, Behnisch B, Dirschinger J, Wintermantel E, Schömig A; investigators of the individualizable durg-eluting Stent System to Abrogate Restenosis Project. Prevention of restenosis by a novel drug-eluting stent system with a dose-adjustable, polymer-free, on-site stent coating. Eur Heart J 2005; 26: 1475-1481.

[5] Mehilli J, Kastrati A, Wessely R, Dibra A, Hausleiter J, Jaschke B, Dirschinger J, Schömig A; Intracoronary Stenting and Angiographic Restenosis-Test Equivalence Between 2 Drug-Eluting Stents (ISAR-TEST) Trial Investigators. Randomized trial of a nonpolymer-coated rapamycin-eluting stent versus a polymer-coated paclitaxel-eluting stent for the reduction of late lumen loss. Circulation 2006; 113: 273-279.

[6] Ruef J, Störger H, Schwarz F, Haase J. Comparison of a polymer-free rapamycin-eluting stent (YUKON) with a polymer-coated paclitaxel-eluting stent (TAXUS) in real-world coronary artery lesions. Catheter Cardiovasc Interv 2008; 71: 340-341.

[7] Murata A, Wallace-Bradley D, Tellez A, Alviar C, Aboodi M, Sheehy A, Coleman L, Perkins L, Nakazawa G, Mintz G, Kaluza GL, Virmani R, Granada JF. Accuracy of optical coherence tomography in the evaluation of neointimal coverage after stent implantation. JACC Cardiovasc Imaging 2010; 3: 76-84.

[8] Templin C, Meyer M, Müller MF, Djonov V, Hlushchuk R, Dimova I, Flueckiger S, Kronen P, Sidler M, Klein K, Nicholls F, Ghadri JR, Weber K, Paunovic D, Corti R. Coronary optical frequency domain imaging (OFDI) for in vivo evaluation of stent healing: comparison with light and electron microscopy. Eur Heart J 2010; 31: 1792-1801.

[9] Jang IK, Bouma BE, Kang DH, Park SJ, Park SW, Seung KB, Choi KB, Shishkov M, Schlendorf K, Pomerantsev E, Houser SL, Aretz HT, Tearney GJ. Visualization of coronary atherosclerotic plaques in patients using optical coherence tomography: comparison with intravascular ultrasound. J Am Coll Cardiol 2002; 39: 604-609.

[10] Coletta J, Suzuki N, Nascimento BR, Bezerra HG, Rosenthal N, Guagliumi G, Rollins AM, Costa MA. Use of optical coherence tomography for accurate characterization of atherosclerosis. Arq Bras Cardiol 2010; 94: 250-4, 268-72, 254-259.

[11] Tearney GJ, Waxman S, Shishkov M, Vakoc BJ, Suter MJ, Freilich MI, Desjardins AE, Oh WY, Bartlett LA, Rosenberg M, Bouma BE. Three-dimensional coronary artery microscopy by intracoronary optical frequency domain imaging. JACC Cardiovasc Imaging 2008; 1: 752-761.

[12] Her AY, Kim JS, Kim YH, Shin DH, Kim BK, Ko YG, Choi D, Jang Y, Hong MK. Histopathologic validation of optical coherence tomography findings of non-apposed side-branch struts in porcine arteries. J Invasive Cardiol 2013; 25: 364-366.

[13] Kim JS, Afari ME, Ha J, Tellez A, Milewski K, Conditt G, Cheng Y, Hua Yi G, Kaluza GL, Granada JF. Neointimal patterns obtained by optical coherence tomography correlate with specific histological components and neointimal proliferation in a swine model of restenosis. Eur Heart J Cardiovasc Imaging 2014; 15: 292-298.

[14] Guagliumi G, Musumeci G, Sirbu V, Bezerra HG, Suzuki N, Fiocca L, Matiashvili A, Lortkipanidze N, Trivisonno A, Valsecchi O, Biondi-Zoccai G, Costa MA; ODESSA Trial Investigators. Optical coherence tomography assessment of in vivo vascular response after implantation of overlapping bare-metal and drug-eluting stents. JACC Cardiovasc Interv 2010; 3: 531-539.

[15] Gonzalo N, Serruys PW, Okamura T, van Beusekom HM, Garcia-Garcia HM, van Soest G, van der Giessen W, Regar E. Optical coherence tomography patterns of stent restenosis. Am Heart J 2009; 158: 284-293.

[16] Bland JM, Altman DG. Statistical methods for assessing agreement between two methods of clinical measurement. Lancet 1986; 1: 307-310.

[17] Chen BX, Ma FY, Luo W, Ruan JH, Xie WL, Zhao XZ, Sun SH, Guo XM, Wang F, Tian T, Chu XW. Neointimal coverage of bare-metal and sirolimus-eluting stents evaluated with optical coherence tomography. Heart 2008; 94: 566-570.

[18] Fu Q, Suzuki N, Kozuma K, Miyagawa M, Nomura T, Kawashima H, Shiratori Y, Ishikawa S, Kyono H, Isshiki T. Quantitative optical coherence tomography analysis for late in-stent restenotic lesions. Int Heart J 2015; 56: 13-17.

[19] Lemos PA, Takimura CK, Laurindo FR, Gutierrez PS, Aiello VD. A histopathological comparison of different definitions for quantifying instent neointimal tissue: implications for the validity of intracoronary ultrasound and optical coherence tomography measurements. Cardiovasc Diagn Ther 2011; 1: 3-10.

[20] Farooq V, Serruys PW, Heo JH, Gogas BD, Onuma Y, Perkins LE, Diletti R, Radu MD, Räber L, Bourantas CV, Zhang Y, van Remortel E, Pawar R, Rapoza RJ, Powers JC. Intracoronary optical

coherence tomography and histology of overlapping everolimus-eluting bioresorbable vascular scaffolds in a porcine coronary artery model: the potential implications for clinical practice. JACC Cardiovasc Interv 2013; 6: 523-532.

[21] Tearney GJ, Yabushita H, Houser SL, Aretz HT, Jang IK, Schlendorf KH, Kauffman CR, Shishkov M, Halpern EF, Bouma BE. Quantification of macrophage content in atherosclerotic plaques by optical coherence tomography. Circulation 2003; 107: 113-119.